

# 000 001 002 003 004 005 006 007 008 009 010 011 012 013 014 015 016 017 018 019 020 021 022 023 024 025 026 027 028 029 030 031 032 033 034 035 036 037 038 039 040 041 042 043 044 045 046 047 048 049 050 051 052 053 MULTI-VIEW GRAPH DISENTANGLEMENT VIA JOINT CONTRASTIVE OPTIMIZATION

Anonymous authors

Paper under double-blind review

## ABSTRACT

Graph Representation Learning (GRL) has made great progress by optimizing node representations through constructing multiple views and employing mutual information maximization or contrastive learning methods. However, existing methods typically rely on graph augmentation to construct node- and graph-level views by maximizing inter-view consistency. This strategy tends to force different views toward homogeneity, and may discard critical information in the graph data. Meanwhile, views at different hierarchical levels exhibit inherent limitations: node-level views are sensitive to noise, and graph-level views overlook local structural information. In this work, we propose **Multi-view Graph Representation Learning with Disentanglement via joint contrastive optimization (MGDRL)**. Multi-view graph disentanglement (MGD) promotes divergence among representations across different views, forming decoupled views. However, disentanglement alone may lead to meaningless representations. Therefore, we employ fuzzy self-attention mechanism to construct an aggregation graph and achieve synergistic constraints between the aggregation graph and MGD through joint contrastive optimization. Joint contrastive optimization guides decoupled views toward distinct and diverse information while also extending contrastive learning to the subgraph-level of the aggregation graph, integrating local and global information. Experimental results on benchmark datasets demonstrate the superior performance of MGDRL.

## 1 INTRODUCTION

Graph Neural Networks (GNNs) propagate information between nodes through a message-passing mechanism, modeling local structural patterns, and have demonstrated exceptional performance in tasks such as node classification (Shen et al., 2025), link prediction (Cai et al., 2021), and graph classification (Zhang et al., 2018). Most existing GNNs are trained in a supervised manner, but they often rely on large amounts of labeled data, which limits their applicability in tasks such as protein function prediction (Zhang et al., 2024c) where expert annotations are scarce, and as network depth increases, they become prone to over-smoothing, reducing their discriminative ability (Li et al., 2018).

Graph Representation Learning (GRL) combines view-invariance learning with graph structural properties (Zhao et al., 2025), using self-supervised methods to extract salient information from the data and thereby reduce the model’s dependence on labeled examples. As one of the core paradigms of GRL, Graph Contrastive Learning (GCL) aims to learn representations by constructing different views of samples and comparing positive and negative instances in the embedding space (Zhang et al., 2023; Li et al., 2023; Zhang et al., 2024a).

To enhance the generalization and robustness of representation learning on graph-structured data, GCL employs various graph augmentation techniques to generate augmented views (Ding et al., 2022), such as feature masking (Zhu et al., 2021; You et al., 2020), edge perturbationRong et al. (2020), node dropping (You et al., 2020), subgraph samplingQiu et al. (2020). After obtaining different views, most GCL methods learn discriminative and invariant essential representations in graph data by maximizing mutual information (Veličković et al., 2019). Mutual information maximization methods can be categorized into two types (Zhao et al., 2025). The first (Veličković et al., 2019; Peng et al., 2020; Zhao et al., 2023) constructs positive and negative sample pairs between

054 node representations and a global graph or a local summary. The second maximizes a lower bound  
 055 on mutual information (Gutmann & Hyvärinen, 2010; Oord et al., 2018; Sohn, 2016). Despite the  
 056 flourishing development of GCL, this paradigm still has some drawbacks.

057 Theoretical and empirical research both indicate that effective augmented views should exhibit diversity  
 058 while preserving the integrity of task-relevant information (Tian et al., 2020; Gong et al., 2023).  
 059 However, most existing GCL methods employ manual graph augmentation strategies (Ding et al.,  
 060 2022), which cannot guarantee that task-relevant information is preserved and may even severely dis-  
 061 rupt graph topologies highly related to downstream tasks, resulting in low-quality embeddings (Zhu  
 062 et al., 2021).

063 On the other hand, existing GCL methods focus on generating node- and graph-level contrastive  
 064 views (Zhao et al., 2025). Node-level views can effectively capture feature information for individual  
 065 nodes. However, they are highly sensitive to feature perturbations and node noise (Ju et al., 2024).  
 066 Graph-level views provide a global representation, but because they rely on global pooling, they  
 067 struggle to preserve structural patterns such as functional modules or intra-community dependencies,  
 068 resulting in ambiguity in local semantics (Ying et al., 2018). In addition, existing GCL methods treat  
 069 corresponding nodes across different views as positive pairs (Shen et al., 2023), which drives the  
 070 representations of the views to converge toward similarity and fails to fully exploit the multi-view  
 071 capacity to capture diverse representations.

072 To obtain more diverse representations without applying graph perturbations and to overcome the  
 073 limitations of contrastive views, we propose MGDRL, a graph representation learning framework  
 074 that performs multi-view graph disentanglement (MGD) via joint contrastive optimization. In MG-  
 075 DRL, we employ MGD to generate three decoupled views of graph data, enabling diverse repre-  
 076 sentations across the decoupled views without compromising critical graph information. However,  
 077 the driving force provided by disentanglement alone is insufficient and may lead to meaningless  
 078 representations. Therefore, we propose joint contrastive optimization, utilizing contrastive learning  
 079 as a constraint for MGD to drive decoupled views to learn diverse semantic information. First, we  
 080 aggregate the decoupled views through fuzzy self-attention to obtain the aggregation graph. Based  
 081 on their distinct roles in the aggregation process, these decoupled views are designated as the *transi-*  
 082 *tion* (*t*), *readout* (*r*) and *embedding* (*e*) views, respectively. Then, we use the aggregation graph and  
 083 decoupled view *e* as contrastive objectives to perform node-subgraph and subgraph-subgraph level  
 084 comparisons, which we refer to as subgraph contrastive learning. Using joint contrastive optimiza-  
 085 tion not only encourages the decoupled views to focus on distinct and diverse information, but also  
 086 extends the contrastive objective to subgraph-level views, thereby achieving a integration between  
 087 local and global information. The main contributions of this work are as follows:

- 088 • We construct MGD to obtain decoupled views that capture diverse information without  
 089 graph augmentation.
- 090 • We propose subgraph contrastive learning, which extends the contrastive objective to the  
 091 node-subgraph and subgraph-subgraph levels, enabling the aggregation graph to integrate  
 092 local and global information.
- 093 • We propose joint contrastive optimization, which uses fuzzy self-attention aggregation as  
 094 a bridge between MGD and subgraph contrastive learning, to obtain diverse information  
 095 across decoupled views and comprehensive node- and graph-level representations in the  
 096 aggregation graph.
- 097 • Experimental results on multiple datasets show that MGDRL performs excellently on semi-  
 098 supervised node classification and node clustering tasks, even outperforming some super-  
 099 vised GNNs.

## 101 2 RELATED WORK

102 **Graph Augmentation** In GRL, before performing contrastive learning, the original graph is aug-  
 103 mented in various ways to obtain multiple augmented views. For example, GraphCL (You et al.,  
 104 2020) systematically introduced four basic augmentation operations, namely feature masking (Zhu  
 105 et al., 2021; You et al., 2020), edge perturbation (Rong et al., 2020), node dropping (You et al.,  
 106 2020) and subgraph sampling (Qiu et al., 2020), to construct augmented views. GRACE (Zhu et al.,  
 107 2020) and CCA-SSG (Zhang et al., 2021) use random edge perturbation and feature masking to

108 generate two views. MVGRL (Hassani & Khasahmadi, 2020) constructs augmented views using  
 109 graph diffusion. SubgDiff (Zhang et al., 2024b) incorporates molecular subgraph information into  
 110 diffusion to enhance the awareness of the denoising network of molecular substructures. To better  
 111 align graph augmentations with downstream tasks, adaptive augmentation methods have gradually  
 112 emerged. GCA (Zhu et al., 2021) applies selective augmentations based on graph structure and node  
 113 feature importance, assigning higher masking probability to less important elements. AutoGCL (Yin  
 114 et al., 2022) adjusts perturbation strength dynamically to balance diversity and the integrity of task-  
 115 relevant information. GOUDA (Zhudo et al., 2024) employs a learnable unified graph augmentation  
 116 module to simulate arbitrary explicit graph augmentations. To avoid information loss and reduced  
 117 generalization from handcrafted augmentations, GraphACL (Xiao et al., 2023) captures 1-hop local  
 118 neighborhood information and two-hop monophily similarity without augmentation. S3GCL (Wan  
 119 et al., 2024) generates low-pass and high-pass biased views using cosine parameterized Chebyshev  
 120 polynomial filters.

121 **Contrastive Methods** The contrastive method in GRL comprises two components, contrastive  
 122 views and contrastive objectives. Contrastive views determine the structural and semantic levels the  
 123 model can capture, while contrastive objectives determine how the model measures sample similar-  
 124 ity and carries out optimization (Zhao et al., 2025). Contrastive objectives primarily focus on com-  
 125 parisons at the node-node and node-graph levels (Xie et al., 2022). At the node-graph level, methods  
 126 commonly optimize local-global mutual information using the Bayes–Shannon lower bound or the  
 127 Jensen–Shannon divergence. For instance, DGI (Veličković et al., 2019) maximizes the mutual in-  
 128 formation between the node embeddings of the original graph and the global graph summary and  
 129 uses the corrupted graph as the negative sample. MVGRL (Hassani & Khasahmadi, 2020) performs  
 130 multi-view contrast by comparing two sets of node-level views with the global graph summary in  
 131 order to maximize inter-view mutual information. Node-node level contrast typically uses noise  
 132 contrastive estimation (InfoNCE) or normalized temperature-scaled cross-entropy (NT-Xent) loss  
 133 to bring positive sample pairs closer in the embedding space while pushing negative sample pairs  
 134 farther apart. For example, NCLA (Shen et al., 2023) introduces a neighbor contrastive loss that  
 135 regards the anchor and its neighbor nodes across different augmented node views as positive pairs,  
 136 and all other nodes as negative pairs. GTCA (Liang et al., 2025) proposes a multi-positive sample  
 137 contrastive loss that uses the intersection of  $k$  nearest neighbor sets from multiple views as positive  
 138 samples, treating all remaining samples as negative samples.

### 139 3 PRELIMINARIES

140 Let  $\mathcal{G} = (\mathcal{V}, \mathcal{E})$  denote a graph, where  $\mathcal{V} = \{v_1, \dots, v_N\}$ ,  $\mathcal{E} \subseteq \mathcal{V} \times \mathcal{V}$  represent the node set and  
 141 the edge set respectively.  $\mathbf{X} \in \mathbb{R}^{N \times F}$  and  $\mathbf{A} \in \{0, 1\}^{N \times N}$  denote the node feature matrix and the  
 142 symmetric adjacency matrix, where  $\mathbf{x}_i \in \mathbb{R}^F$  is the feature vector of  $v_i$  and  $A_{ij} = 1$  iff  $(v_i, v_j) \in \mathcal{E}$ ,  
 143 otherwise  $A_{ij} = 0$ .  $\mathcal{N}_i$  represents the first-order neighbors of node  $i$  in the graph.  $\mathcal{S}_i = \mathcal{N}_i \cup \{v_i\}$   
 144 denotes the subgraph centered on node  $i$  and containing its 1-hop neighbors. Given  $\mathbf{X}$  and  $\mathbf{A}$  as  
 145 the input, the proposed model employs the GNN encoder  $f(\mathbf{X}, \mathbf{A})$  to learn the representations of  
 146 nodes  $\mathbf{H} = f(\mathbf{X}, \mathbf{A}) \in \mathbb{R}^{N \times F'}$ ,  $F' \ll F$ . The aggregation graph is generated by aggregating the  
 147 decoupled views. These views are learned by optimizing the joint contrastive loss, without access to  
 148 the labels of downstream tasks.

### 151 4 METHODOLOGY

152 In this section, we describe the MGDRL in detail from three perspectives, including multi-view  
 153 graph disentanglement, fuzzy self-attention aggregation and subgraph contrastive learning. Finally,  
 154 we analyze the time complexity of MGDRL. Figure 1 shows the overall architecture of MGDRL.

#### 157 4.1 MULTI-VIEW GRAPH DISENTANGLEMENT

158 Graph disentanglement can promote the distinctiveness and diversity of the decoupled views, with-  
 159 out relying on any prior knowledge or manually defined data augmentation strategies. In MGDRL,  
 160 we employ multi-view graph disentanglement (MGD) to generate three decoupled views for all  
 161 benchmark datasets. Based on their respective functions described in the Section 4.2, we designate

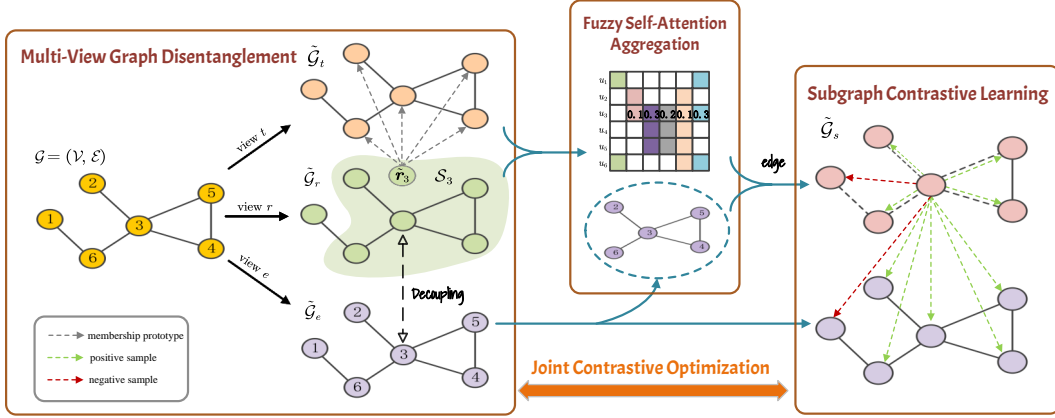


Figure 1: The overall architecture of MGDR. The original graph generates three decoupled views  $t, r$  and  $e$  via MGD. For each subgraph  $\mathcal{S}_i$ , the fuzzy self-attention weights are computed from the fuzzy membership between the local readout of view  $r$  and the subgraph’s nodes in view  $t$ . Then, the fuzzy self-attention aggregation is performed on view  $e$  to produce aggregation graph ( $s$ ) and the subgraph contrastive learning is conducted between view  $e$  and view  $s$ . Finally, we employ MGD and subgraph contrastive learning to jointly optimize the aggregation graph and decoupled views.

the three decoupled views as *transition* ( $t$ ), *readout* ( $r$ ) and *embedding* ( $e$ ). For each decoupled view  $z \in \{t, r, e\}$ , the edge coefficient between two connected nodes, say  $v_i$  and  $v_j$ , can be learned as

$$\alpha_{ij}^z = \frac{\exp(\text{LeakyReLU}_\rho(\mathbf{a}_z[\mathbf{W}_z \mathbf{x}_i \| \mathbf{W}_z \mathbf{x}_j]))}{\sum_{v_p \in \mathcal{S}_i} \exp(\text{LeakyReLU}_\rho(\mathbf{a}_z[\mathbf{W}_z \mathbf{x}_i \| \mathbf{W}_z \mathbf{x}_p]))}, \quad (1)$$

where  $\alpha_{ij}^z = 0$  if  $A_{ij} = 0$ ,  $\mathbf{a}_z \in \mathbb{R}^{2F'}$  is the learnable attention vector of the head  $z$ ,  $\mathbf{W}_z \in \mathbb{R}^{F' \times F}$  is the learnable weight matrix of the head  $z$  which maps each input node feature  $\mathbf{x}_i \in \mathbb{R}^F$  to an  $F'$ -dimensional hidden representation,  $\|$  is the concatenation operation, and  $\text{LeakyReLU}_\rho(\cdot)$  is the LeakyReLU nonlinearity with negative slope  $\rho$ . Then, representation diffusion over the adjacency matrix is employed to capture the local readout of view  $r$ , as

$$\tilde{\mathbf{R}} = \widehat{\mathbf{D}}^{-1} \widehat{\mathbf{A}} \mathbf{H}_r, \quad (2)$$

where  $\tilde{\mathbf{R}} \in \mathbb{R}^{N \times F'}$  is the local readout matrix of the view  $r$ ,  $\mathbf{H}_r$  is the embedding matrix of view  $r$ ,  $\widehat{\mathbf{A}} = \mathbf{A} + \mathbf{I}_N \in \mathbb{R}^{N \times N}$  is the adjacency matrix augmented with self-loops,  $\widehat{\mathbf{D}}_{i,i} = \sum_{j=1}^N \widehat{\mathbf{A}}_{i,j}$  is the corresponding degree matrix.

**Graph disentanglement loss.** Using the local readout  $\tilde{\mathbf{r}}$  as an anchor, we simultaneously maximize its similarity with the embedding of view  $r$  and minimize its similarity with the embedding of view  $e$ . This contrasting constraint forces the embeddings of view  $r$  and view  $e$  to separate in the vector space, thereby reducing their inter-view correlation and achieving graph disentanglement. The graph disentanglement loss is defined as

$$\mathcal{L}_d = -\frac{1}{N} \sum_{i=1}^N \left[ \log \sigma(\varphi(\tilde{\mathbf{r}}_i, \mathbf{h}_i^r)) + \log(1 - \sigma(\varphi(\tilde{\mathbf{r}}_i, \mathbf{h}_i^e))) \right], \quad (3)$$

where  $\tilde{\mathbf{r}}_i$  is the local readout for node  $i$  of the decoupled view  $r$ ,  $\varphi(\mathbf{u}, \mathbf{v}) = \mathbf{u}^\top \mathbf{W}_d \mathbf{v}$  is a bilinear discriminator with parameters  $\mathbf{W}_d \in \mathbb{R}^{F' \times F'}$ ,  $\sigma(\cdot)$  is a sigmoid function.  $\mathbf{h}_i^r$  and  $\mathbf{h}_i^e$  are the embeddings of node  $i$  in view  $r$  and view  $e$ , respectively.

## 4.2 FUZZY SELF-ATTENTION AGGREGATION

After obtaining the decoupled views, we aggregate these views into an aggregation graph, which serves as a bridge for the joint contrastive optimization of MGD and subgraph contrastive learning (described in Section 4.3). Considering the fuzzy and overlapping nature of community structure in

graphs, we adopt local membership degrees as fuzzy self-attention weights to aggregate the decoupled views into the aggregation graph. In this approach, we assign three decoupled views distinct roles: view  $t$  serves as the foundational view to obtain basic features, while view  $r$  provides local readout for computing fuzzy self-attention weights. The node embeddings of view  $e$  are then aggregated using the fuzzy self-attention weights to yield the embeddings of the aggregation graph.

Specifically, in view  $t$ , each node  $j \in \mathcal{S}_i$  acts as a membership prototype, and the local readout vector  $\tilde{\mathbf{r}}_i$  serves as the query to be assigned. The fuzzy self-attention weight is then defined as

$$u_{ij} = \frac{\|\tilde{\mathbf{r}}_i - \mathbf{h}_j^t\|_2^{-\frac{2}{m-1}}}{\sum_{k \in \mathcal{S}_{(i)}} \|\tilde{\mathbf{r}}_i - \mathbf{h}_k^t\|_2^{-\frac{2}{m-1}}} \quad , \quad (4)$$

where  $\sum_{j \in \mathcal{S}_i} u_{ij} = 1$ ,  $\|\cdot\|_2$  is the  $L^2$  norm,  $m$  is the fuzziness weighting exponent that controls the fuzziness degree of clustering outcomes.

Then, we aggregate the node embeddings in view  $e$  by the fuzzy self-attention weights to obtain the embeddings of aggregation graph, which we denote as  $s$ . Although there are no explicit edge relationships between the embeddings of aggregation graph, the homophily principle of networks suggests that similar subgraphs are closely related (McPherson et al., 2001). In MGDRL, we consider subgraph pairs with intersections as “closely connected subgraphs” and establish an edge between their embedding pairs. The embedding for each subgraph is obtained as

$$\mathbf{h}_i^s = \sum_{j \in \mathcal{S}_{(i)}} u_{ij} \mathbf{h}_j^e \quad . \quad (5)$$

The edge relationship of the aggregation graph is defined as  $\tilde{\mathcal{E}}_s = \{(\mathbf{h}_i^s, \mathbf{h}_j^s) \mid \mathcal{S}_i \cap \mathcal{S}_j \neq \emptyset, i \neq j\}$ , and the set of subgraphs that intersect with subgraph  $i$  is defined as  $\mathcal{P}_i = \{\mathcal{S}_j \mid \mathcal{S}_i \cap \mathcal{S}_j \neq \emptyset, i \neq j\}$ . Since  $\mathcal{S}_i$  is a 1-hop neighborhood subgraph for node  $i$ , its adjacency matrix coincides exactly with that of the original graph  $\mathcal{G}$ , i.e.,  $\tilde{\mathbf{A}}_s = \mathbf{A} \in \{0, 1\}^{N \times N}$ . Then, the aggregation graph can be defined as  $\tilde{\mathcal{G}}_s = (\mathbf{H}_s, \tilde{\mathbf{A}}_s, \tilde{\mathcal{E}}_s)$ .

#### 4.3 SUBGRAPH CONTRASTIVE LEARNING

Our experiments indicate that a single graph disentanglement loss does not provide sufficient guidance for the model to generate meaningful features. Therefore, it is necessary to combine disentanglement with other pretext tasks to constrain the correlations among the decoupled views. To address these issues, we propose subgraph contrastive learning. Traditional node-node and node-graph level contrastive learning methods suffer from limitations such as node-level noise and the lack of localized structural features. The proposed subgraph contrastive learning extends the contrastive objective to the subgraph-level and achieves a integration between local and global information.

**Subgraph contrastive loss.** Subgraph contrastive learning uses subgraph-level and node-level views for intra-view and inter-view comparison. Therefore, the aggregation graph embedding  $\mathbf{h}_i^s$  derives its positive samples from two sources:

- $\{\mathbf{h}_j^s \mid \mathcal{S}_j \in \mathcal{P}_i\}$ , the aggregation graph embedding of the subgraph  $j$  that intersects subgraph  $i$ .
- $\{\mathbf{h}_k^e \mid v_k \in \mathcal{S}_i\}$ , the node embedding of the node  $k$  contained in subgraph  $i$ .

Then, the intra-view subgraph contrastive loss, which can be regarded as subgraph-subgraph level comparison, can be formulated as

$$\ell_{intra}(\mathbf{h}_i^s) = -\log \frac{\sum_{v_k \in \mathcal{N}_i} \exp(\theta(\mathbf{h}_i^s, \mathbf{h}_k^s)/\tau)}{\sum_{i \neq j} \exp(\theta(\mathbf{h}_i^s, \mathbf{h}_j^s)/\tau)} \quad , \quad (6)$$

and the inter-view subgraph contrastive loss, which can be regarded as node-subgraph level comparison, can be formulated as

$$\ell_{inter}(\mathbf{h}_i^s) = -\log \frac{\sum_{v_k \in \mathcal{S}_i} \exp(\theta(\mathbf{h}_i^s, \mathbf{h}_k^e)/\tau)}{\sum_j \exp(\theta(\mathbf{h}_i^s, \mathbf{h}_j^e)/\tau)} \quad , \quad (7)$$

270 where  $\tau$  is a temperature parameter,  $\theta(\cdot)$  is the cosine similarity. The terms in the denominator of  
 271 Eq. (6) and Eq. (7) can be decomposed as  
 272

$$\sum_{i \neq j} \exp(\theta(\mathbf{h}_i^s, \mathbf{h}_j^s)/\tau) = \underbrace{\sum_{\mathcal{S}_j \in \mathcal{P}_i} \exp(\theta(\mathbf{h}_i^s, \mathbf{h}_j^s)/\tau)}_{\text{intra-view pos}} + \underbrace{\sum_{\mathcal{S}_j \notin \mathcal{P}_i} \exp(\theta(\mathbf{h}_i^s, \mathbf{h}_j^s)/\tau)}_{\text{intra-view neg}},$$

$$\sum_j \exp(\theta(\mathbf{h}_i^s, \mathbf{h}_j^e)/\tau) = \underbrace{\sum_{v_j \in \mathcal{S}_i} \exp(\theta(\mathbf{h}_i^s, \mathbf{h}_j^e)/\tau)}_{\text{inter-view pos}} + \underbrace{\sum_{v_j \notin \mathcal{S}_i} \exp(\theta(\mathbf{h}_i^s, \mathbf{h}_j^e)/\tau)}_{\text{inter-view neg}},$$

273 where the non-connected aggregation graph embeddings and non-containing nodes of subgraph  $i$   
 274 are regarded as negative pairs, respectively. Minimizing Eq. (6) and Eq. (7) would maximize the  
 275 agreement between positive pairs and minimize that of negative pairs. The final subgraph contrastive  
 276 loss is defined as  
 277

$$\mathcal{L}_s = \frac{1}{N} \sum_{i=1}^N (\ell_{\text{intra}}(\mathbf{h}_i^s) + \ell_{\text{inter}}(\mathbf{h}_i^s)). \quad (8)$$

278 **Joint contrastive optimization.** Joint contrastive optimization is a dynamic and coordinated  
 279 process between MGD and subgraph contrastive learning. Connected via fuzzy self-attention aggre-  
 280 gation, MGD produces distinct and diverse decoupled views, while subgraph contrastive learning  
 281 simultaneously constrains MGD and enables these views to integrate both local and global infor-  
 282 mation. The final joint contrastive loss is defined as  
 283

$$\mathcal{L}_J = \mathcal{L}_d + \lambda \cdot \mathcal{L}_s \quad , \quad (9)$$

284 where  $\lambda$  is a tunable constraint weight parameter.  
 285

#### 286 4.4 TIME COMPLEXITY

287 For MGD to produce  $K$  views, the time complexity is  $\mathcal{O}((NFF' + |\mathcal{E}|F')K)$ , where  $N$  and  $|\mathcal{E}|$   
 288 are the number of nodes and edges in graph  $\mathcal{G}$ , with  $F$  and  $F'$  denoting the input feature dimension  
 289 and the output embedding dimension. The time complexity of the graph disentanglement loss is  
 290  $\mathcal{O}(NF'^2 + |\mathcal{E}|F')$ . Let  $M = \frac{|\mathcal{E}|}{N}$  denote the average node degree, the time complexity of fuzzy  
 291 self-attention aggregation is  $\mathcal{O}(NMF')$  and the time complexity of subgraph contrastive learning is  
 292  $\mathcal{O}(N(M+N)F')$ . Thus, the time complexity of MGDRL is  $\mathcal{O}(NFF'K + |\mathcal{E}|F'(K+1) + NF'^2 +$   
 293  $N(M+N)F')$ . Since  $|\mathcal{E}| \ll N^2$  and  $M \ll F' \ll F$ , the overall time complexity of MGDRL is  
 294  $\mathcal{O}(NFF'K + N^2F')$ . Note  $K$  is very small (e.g., 3) in our experiments, so the time complexity  
 295 of MGDRL is comparable to the representative node-node GRL methods, e.g., GRACE (Zhu et al.,  
 296 2020).

## 307 5 EXPERIMENTS

### 308 5.1 DATASETS

309 In our experiments, we evaluate our method on seven widely-used datasets for semi-supervised node  
 310 classification, including three citation networks, i.e., Cora, Citeseer, Pubmed (Sen et al., 2008), a  
 311 reference network constructed based on Wikipedia, i.e., Wiki-CS (Mernyei & Cangea, 2020), a co-  
 312 authorship network, i.e., Coauthor-CS (Shchur et al., 2018), and two product co-purchase networks,  
 313 i.e., Amazon-Computers and Amazon-Photo (Shchur et al., 2018). Datasets Cora, Citeseer and  
 314 Pubmed were also used to evaluate performance on the node clustering task.  
 315

### 316 5.2 BASELINES

317 We thoroughly consider 20 state-of-the-art methods for comparison on semi-supervised node clas-  
 318 sification and node clustering tasks. Baselines trained with labels: GCN (Kipf & Welling, 2017),  
 319 GAT (Velickovic et al., 2017), CGPN (Wan et al., 2021b), CG3 (Wan et al., 2021a). Baselines  
 320 trained without labels: DGI (Veličković et al., 2019), GMI (Peng et al., 2020), MVGRL (Hassani &  
 321 Khasahmadi, 2020), GRACE (Zhu et al., 2020), GCA (Zhu et al., 2021), ProGCL (Xia et al., 2021),

324 Table 1: Node classification performance.  $X, A, Y$  denote the node attributes, adjacency matrix,  
 325 and labels in the datasets.  $S, E$  denote the diffusion matrix and edge feature matrix. OOM signifies  
 326 out-of-memory.

328 329 330 331 332 333 334 335 336 337 338 339 340 341 342 343 344	328 329 330 331 332 333 334 335 336 337 338 339 340 341 342 343 344	328 329 330 331 332 333 334 335 336 337 338 339 340 341 342 343 344	Datasets						
			Cora	Citeseer	Pubmed	CS	Photo	Computers	WikiCS
GCN	$X, A, Y$	79.6±1.8	66.0±1.2	79.0±2.5	90.0±0.6	86.3±1.6	76.4±1.8	67.3±1.5	
GAT	$X, A, Y$	81.2±1.6	68.9±1.8	78.5±1.8	90.9±0.7	86.5±2.1	77.9±1.8	68.6±1.9	
CGPN	$X, A, Y$	74.0±1.7	63.7±1.6	73.3±2.5	83.5±1.4	84.1±1.5	74.7±1.3	66.1±2.1	
CG3	$X, A, Y$	80.6±1.6	70.9±1.5	78.9±2.6	90.6±1.0	89.4±1.9	77.8±1.7	68.0±1.5	
DGI	$X, A$	82.1±1.3	71.6±1.2	78.3±2.4	92.0±0.5	83.5±1.2	78.8±1.1	69.1±1.4	
GMI	$X, A$	79.4±1.2	66.9±2.2	76.8±2.3	88.5±0.8	86.7±1.5	76.1±1.2	67.8±1.8	
MVGRL	$X, S, A$	82.4±1.5	71.1±1.4	79.5±2.2	91.5±0.6	89.7±1.2	78.7±1.7	69.2±1.2	
GRACE	$X, A$	79.6±1.4	67.0±1.7	74.6±3.5	90.0±0.7	87.9±1.4	76.8±1.7	67.8±1.4	
GCA	$X, A$	79.0±1.4	65.6±2.4	81.5±2.5	90.9±1.1	87.0±1.9	76.9±1.4	67.6±1.3	
AFGRL	$X, A$	78.6±1.3	70.8±2.1	76.4±2.5	91.4±0.6	89.2±1.1	77.7±1.1	68.0±1.7	
SUGRL	$X, A$	81.3±1.2	71.0±1.8	80.5±1.6	91.2±0.9	90.5±1.9	78.2±1.2	68.7±1.1	
ARIEL	$X, A$	81.3±1.3	70.9±1.4	74.2±2.5	90.2±0.9	90.6±1.8	81.3±1.4	70.5±2.1	
NCLA	$X, A$	82.2±1.6	71.7±0.9	82.0±1.4	91.5±0.7	90.2±1.3	79.8±1.5	70.3±1.7	
GraphACL	$X, A$	82.0±1.1	71.5±1.4	78.6±1.9	86.9±1.2	90.0±1.0	-	-	
PiGCL	$X, A$	80.0±1.5	71.2±1.1	76.5±3.5	91.0±0.7	71.8±3.4	-	-	
AFECL	$X, E, A$	82.1±1.3	71.3±1.3	81.2±1.7	90.9±1.3	89.2±1.2	-	-	
GTCA	$X, A$	82.5±1.3	68.3±1.4	OOM	<b>92.5±0.6</b>	90.5±1.2	79.2±1.4	69.7±1.5	
MGDRL(Ours)	$X, A$	<b>83.1±1.4</b>	<b>72.3±1.1</b>	<b>82.0±1.2</b>	<b>92.0±0.3</b>	<b>91.4±0.9</b>	<b>81.4±1.4</b>	<b>73.7±1.9</b>	

345  
346 Table 2: Node clustering performance. OOM signifies out-of-memory.

347 348 349 350 351 352 353 354 355 356 357 358 359 360 361	347 348 349 350 351 352 353 354 355 356 357 358 359 360 361	347 348 349 350 351 352 353 354 355 356 357 358 359 360 361	Cora		Citeseer		Pubmed	
			NMI	ARI	NMI	ARI	NMI	ARI
DGI	0.5370	0.4469	0.4185	0.4140	0.3188	0.3165		
GRACE	0.4758	0.3633	0.3960	0.3977	0.3508	0.3286		
GCA	0.4510	0.3104	0.3737	0.3675	0.3307	0.2919		
ProGCL	0.5131	0.3434	0.4115	0.4219	OOM	OOM		
Local-GCL	0.5386	0.4479	0.4508	0.4494	0.3469	0.3304		
AFGRL	0.3525	0.2465	0.3896	0.3958	0.3689	0.2474		
SUGRL	0.2977	0.2766	0.4454	0.4507	0.2977	0.2766		
NCLA	0.6089	0.5750	0.4553	0.4610	0.2523	0.2383		
PiGCL	0.5494	0.4670	0.4581	0.4720	<b>0.3784</b>	<b>0.3612</b>		
UniFilter	0.5212	0.4744	0.4422	0.4318	0.3145	0.2773		
GTCA	0.5588	0.5063	0.3392	0.3125	OOM	OOM		
MGDRL(Ours)	<b>0.6190</b>	<b>0.6076</b>	<b>0.4594</b>	<b>0.4732</b>	0.3643	<u>0.3459</u>		

362 Local-GCL (Zhang et al., 2022), AFGRL (Lee et al., 2022), SUGRL (Mo et al., 2022), ARIEL (Feng  
 363 et al., 2022), NCLA (Shen et al., 2023), GraphACL (Xiao et al., 2023), PiGCL (He et al., 2024),  
 364 UniFilter (Huang et al., 2024), GTCA (Liang et al., 2025), AFECL (Li et al., 2025).

365  
366 5.3 EXPERIMENTAL SETTINGS

367 The proposed MGDRL was implemented using PyTorch 2.5.1 (Paszke et al., 2019) and Deep Graph  
 368 Library 2.0.0 (Wang et al., 2019), and trained by the Adam optimizer on all datasets. For the node  
 369 classification task, we allow GRL baselines and MGDRL to learn embeddings in an unsupervised  
 370 manner, then use these embeddings to train and test a  $L_2$ -regularized logistic regression (LR) clas-  
 371 sifier for semi-supervised node classification. For Cora, Citeseer and Pubmed, we followed (Yang  
 372 et al., 2016) to randomly select 20 nodes per class for training, 500 nodes for validation and the  
 373 remaining nodes for test. For Coauthor-CS and Amazon-Photo, we followed Liu et al. (2020) to  
 374 randomly select 20 nodes per class for training, 30 nodes per class for validation, and the remaining  
 375 nodes for testing. Note that for the GRL baselines and MGDRL, which learn embeddings from un-  
 376 labeled data, the validation set was just used to tune the hyperparameters of the LR classifier, rather  
 377 than the GRL models. For each dataset, we conducted 20 random splits of training/validation/test,  
 378 and reported the averaged performance of all algorithms on the same random splits. For the node

378 Table 3: Ablation study of MGDRL for node classification on all seven datasets.  
379

380 <b>Variants</b>	381 $\mathcal{L}_d$	382 $\mathcal{L}_s$	383 $\mathcal{L}_i$	384 <b>Cora</b>	385 <b>Citeseer</b>	386 <b>Pubmed</b>	387 <b>CS</b>	388 <b>Photo</b>	389 <b>Computers</b>	390 <b>WikiCS</b>
391 Raw data	392	393	394	395 $63.0 \pm 1.7$	396 $51.5 \pm 1.9$	397 $72.5 \pm 2.2$	398 $87.8 \pm 0.7$	399 $87.7 \pm 1.5$	400 $75.8 \pm 1.7$	401 $70.6 \pm 2.4$
402 Variant 1	403 $\checkmark$	404	405	406 $64.8 \pm 1.9$	407 $56.0 \pm 2.0$	408 $72.6 \pm 2.6$	409 $84.7 \pm 1.1$	410 $84.1 \pm 2.2$	411 $73.6 \pm 1.3$	412 $71.8 \pm 1.4$
413 Variant 2	414	415 $\checkmark$	416	417 $81.8 \pm 1.3$	418 $70.4 \pm 1.5$	419 $80.2 \pm 1.9$	420 $90.3 \pm 0.8$	421 $89.9 \pm 2.2$	422 $80.6 \pm 1.5$	423 $71.6 \pm 2.0$
424 Variant 3	425	426 $\checkmark$	427	428 $63.3 \pm 2.1$	429 $66.2 \pm 2.2$	430 $71.8 \pm 2.0$	431 $77.5 \pm 1.3$	432 $78.9 \pm 1.5$	433 $69.4 \pm 2.1$	434 $63.5 \pm 1.8$
435 Variant 4	436	437 $\checkmark$	438 $\checkmark$	439 $76.4 \pm 1.5$	440 $68.8 \pm 1.5$	441 $71.3 \pm 2.3$	442 $80.1 \pm 1.3$	443 $81.5 \pm 1.9$	444 $65.6 \pm 2.2$	445 $59.7 \pm 2.1$
446 MGDRL	447	448 $\checkmark$	449 $\checkmark$	450 $83.1 \pm 1.4$	451 $72.3 \pm 1.1$	452 $82.0 \pm 1.2$	453 $92.0 \pm 0.3$	454 $91.4 \pm 0.9$	455 $81.4 \pm 1.4$	456 $73.7 \pm 1.9$

388  
389 clustering task, we followed He et al. (2024) to directly input the obtained embedding into a ran-  
390 domly initialized K-Means predictor with up to 500 iterations. We ran this process 10 times and  
391 reported the average NMI and ARI.  
392

#### 393 5.4 OVERALL PERFORMANCE 394

395 **Node Classification.** Table 1 presents the node classification accuracy of MGDRL on seven bench-  
396 mark datasets. These node classification results demonstrate MGDRL’s robust performance across  
397 all seven datasets and validate the superiority of MGD with joint contrastive optimization in fea-  
398 ture extraction. Compared to supervised GNNs, our method achieves an average improvement of  
399 3.9% over GCN and GAT. When evaluated against other supervised methods like CGPN and CG3,  
400 MGDRL comprehensively outperforms them with gains of up to 9.1%. In comparison with self-  
401 supervised GRL methods that employ graph augmentation and node- and graph-level contrastive  
402 learning, such as GRACE, NCLA and PiGCL, our approach achieves comprehensive leading per-  
403 formance. MGDRL also maintains advantages over other methods without graph augmentation,  
404 including GraphACL, AFECL and GTCA.  
405

406 **Node Clustering.** Table 2 shows the node clustering performance of MGDRL on the Cora, Cite-  
407 seer and Pubmed datasets. MGDRL demonstrates strong clustering performance on the Cora and  
408 Citeseer datasets, achieving average improvements of 10.33% in NMI and 15.99% in ARI over the  
409 baseline GRACE. MGDRL also achieved the third-best NMI and second-best ARI performance on  
410 Pubmed. Compared to methods without graph augmentation such as GTCA, MGDRL utilizes joint  
411 contrastive learning to enable the representations to integrate local and global information, thereby  
412 facilitating the formation of distinct clusters for nodes with different labels.  
413

#### 414 5.5 ABLATION STUDY 415

416 Table 3 presents the ablation study results of MGDRL on all seven datasets. “Raw data” denotes the  
417 results obtained by directly processing the raw graph data through GAT without any modifications.  
418 Variants 1, 2, and MGDRL demonstrate the impact of MGD ( $\mathcal{L}_d$ ) and subgraph contrastive learning  
419 ( $\mathcal{L}_s$ ) in the joint contrastive optimization. The performance of Variant 1 is highly unstable, with  
420 accuracy significantly decreasing in three datasets compared to the raw data, indicating that MGD  
421 alone fails to effectively capture meaningful representations. To more intuitively illustrate the con-  
422 straining effect of subgraph contrastive learning on MGD, we introduced InfoNCE ( $\mathcal{L}_i$ ) as a control,  
423 resulting in Variants 3 and 4. From Variants 1, 3, and 4, it can be observed that traditional contrastive  
424 learning methods cannot provide effective driving force for MGD, instead, they may even lead to  
425 mutual performance degradation. The ablation results collectively demonstrate the effectiveness of  
426 the joint contrastive optimization.  
427

#### 428 5.6 VISUALIZATION AND HYPERPARAMETER ANALYSIS 429

430 **Visualization.** We use t-SNE (Van der Maaten & Hinton, 2008) for visualization to more intuitively  
431 show the embedding distributions obtained by variants of MGDRL and four other baseline methods  
432 on Cora, as shown in Figure 2. The visualization of Variant 1 also indicates that using MGD alone  
433 leads the model to learn largely uninformative representations. The comparison between Variants  
434 1 and 2 reveals how MGD and subgraph contrastive learning produce different representations:  
435 MGD encourages views to capture disentangled information, resulting in widely dispersed node  
436

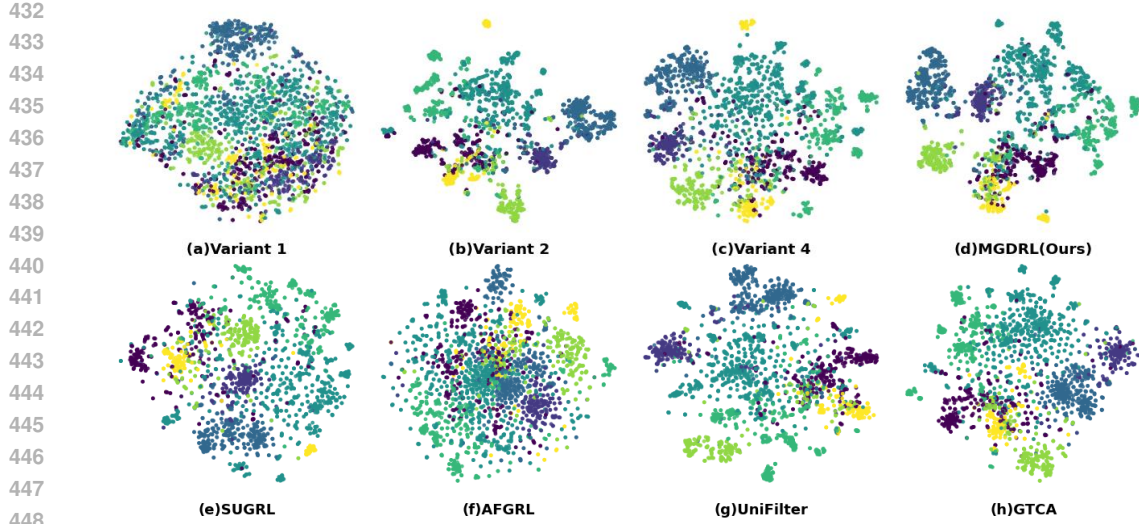
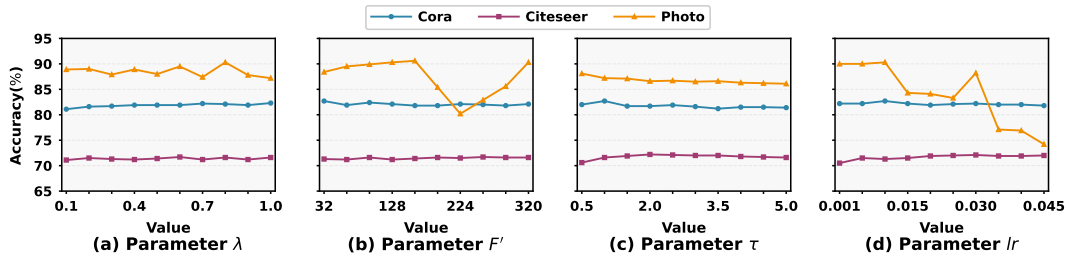


Figure 2: Visualization of variants and four baseline GRL embeddings on Cora with t-SNE.

Figure 3: Sensitivity analysis of the hyperparameters  $\lambda$ ,  $F'$ ,  $\tau$  and  $lr$  on MGDRL.

embeddings, whereas subgraph contrastive learning encourages nodes to integrate local and global information, thereby forming cluster structures. Compared with Variant 4 and the other baselines, MGDRL both pushes nodes of different classes farther apart and preserves cluster structure, which is a consequence of the joint contrastive optimization.

**Hyperparameter analysis.** We conducted sensitivity analysis on Cora, Citeseer, and Photo across four parameters: constraint weight  $\lambda$ , hidden layer dimension  $F'$ , temperature parameter  $\tau$ , and learning rate  $lr$ . The results in Figure 3 demonstrate that MGDRL exhibits highly stable performance on Cora and Citeseer. For the Photo dataset, MGDRL continues to perform well with respect to  $\lambda$  and  $\tau$ . However, performance degradation occurs when using larger values for  $F'$  and  $lr$ .

## 6 CONCLUSION

Existing GRL methods employ graph augmentation to construct views and utilize node- and graph-level contrastive learning for optimization. However, artificial perturbations result in the loss of critical information in graph data, while node- and graph-level contrastive learning suffers from noise sensitivity and an inability to perceive local structure. To address these issues, we propose MGDRL, a graph representation learning framework that performs MGD via joint contrastive optimization. MGD generates decoupled views, which are used to generate the aggregation graph by fuzzy self-attention aggregation. Then, the decoupled view (*embedding*) and the aggregation graph are used for node-subgraph and subgraph-subgraph level comparisons in subgraph contrastive learning. By jointly optimizing the MGD and subgraph contrastive learning, the decoupled views learn distinct and diverse representations, while the aggregation graph integrates both local and global information. Experiments on benchmark datasets demonstrate the effectiveness of MGDRL.

486 REFERENCES  
487

488 Lei Cai, Jundong Li, Jie Wang, and Shuiwang Ji. Line graph neural networks for link prediction.  
489 *IEEE Transactions on Pattern Analysis and Machine Intelligence*, 44(9):5103–5113, 2021.

490 Kaize Ding, Zhe Xu, Hanghang Tong, and Huan Liu. Data augmentation for deep graph learning:  
491 A survey. *ACM SIGKDD Explorations Newsletter*, 24(2):61–77, 2022.

492 Shengyu Feng, Baoyu Jing, Yada Zhu, and Hanghang Tong. Adversarial graph contrastive learning  
493 with information regularization. In *Proceedings of the ACM web conference 2022*, pp. 1362–1371,  
494 2022.

495 Xumeng Gong, Cheng Yang, and Chuan Shi. Ma-gcl: Model augmentation tricks for graph con-  
496 trastive learning. In *Proceedings of the AAAI Conference on Artificial Intelligence*, volume 37,  
497 pp. 4284–4292, 2023.

498 Michael Gutmann and Aapo Hyvärinen. Noise-contrastive estimation: A new estimation principle  
500 for unnormalized statistical models. In *Proceedings of the thirteenth international conference on  
501 artificial intelligence and statistics*, pp. 297–304, 2010.

502 Kaveh Hassani and Amir Hosein Khasahmadi. Contrastive multi-view representation learning on  
503 graphs. In *International conference on machine learning*, pp. 4116–4126, 2020.

504 Dongxiao He, Jitao Zhao, Cuiying Huo, Yongqi Huang, Yuxiao Huang, and Zhiyong Feng. A new  
505 mechanism for eliminating implicit conflict in graph contrastive learning. In *Proceedings of the  
506 AAAI Conference on Artificial Intelligence*, volume 38, pp. 12340–12348, 2024.

507 Keke Huang, Yu Guang Wang, Ming Li, and Pietro Lio. How universal polynomial bases enhance  
508 spectral graph neural networks: Heterophily, over-smoothing, and over-squashing. In *Forty-first  
509 International Conference on Machine Learning*, 2024.

510 Wei Ju, Siyu Yi, Yifan Wang, Zhiping Xiao, Zhengyang Mao, Hourun Li, Yiyang Gu, Yifang Qin,  
511 Nan Yin, Senzhang Wang, et al. A survey of graph neural networks in real world: Imbalance,  
512 noise, privacy and ood challenges. *arXiv preprint arXiv:2403.04468*, 2024.

513 Thomas N. Kipf and Max Welling. Semi-supervised classification with graph convolutional net-  
514 works. In *International Conference on Learning Representations*, 2017.

515 Namkyeong Lee, Junseok Lee, and Chanyoung Park. Augmentation-free self-supervised learning  
516 on graphs. In *Proceedings of the AAAI conference on artificial intelligence*, volume 36, pp. 7372–  
517 7380, 2022.

518 Qimai Li, Zhichao Han, and Xiao-Ming Wu. Deeper insights into graph convolutional networks  
519 for semi-supervised learning. In *Proceedings of the AAAI conference on artificial intelligence*,  
520 volume 32, 2018.

521 Yujun Li, Hongyuan Zhang, and Yuan Yuan. Edge contrastive learning: An augmentation-free graph  
522 contrastive learning model. In *Proceedings of the AAAI Conference on Artificial Intelligence*,  
523 volume 39, pp. 18575–18583, 2025.

524 Zhaojian Li, Bin Zhao, and Yuan Yuan. Bio-inspired audiovisual multi-representation integration  
525 via self-supervised learning. In *Proceedings of the 31st ACM International Conference on Multi-  
526 media*, pp. 3755–3764, 2023.

527 Jianqing Liang, Xinkai Wei, Min Chen, Zhiqiang Wang, and Jiye Liang. Gnn-transformer co-  
528 operative architecture for trustworthy graph contrastive learning. In *Proceedings of the AAAI  
529 Conference on Artificial Intelligence*, volume 39, pp. 18667–18675, 2025.

530 Meng Liu, Hongyang Gao, and Shuiwang Ji. Towards deeper graph neural networks. In *Proceedings  
531 of the 26th ACM SIGKDD international conference on knowledge discovery & data mining*, pp.  
532 338–348, 2020.

533 Miller McPherson, Lynn Smith-Lovin, and James M Cook. Birds of a feather: Homophily in social  
534 networks. *Annual review of sociology*, 27(1):415–444, 2001.

540 Péter Mernyei and Cătălina Cangea. Wiki-cs: A wikipedia-based benchmark for graph neural net-  
 541 works. *arXiv preprint arXiv:2007.02901*, 2020.

542

543 Yujie Mo, Liang Peng, Jie Xu, Xiaoshuang Shi, and Xiaofeng Zhu. Simple unsupervised graph rep-  
 544 resentation learning. In *Proceedings of the AAAI conference on artificial intelligence*, volume 36,  
 545 pp. 7797–7805, 2022.

546 Aaron van den Oord, Yazhe Li, and Oriol Vinyals. Representation learning with contrastive predic-  
 547 tive coding. *arXiv preprint arXiv:1807.03748*, 2018.

548

549 Adam Paszke, Sam Gross, Francisco Massa, Adam Lerer, James Bradbury, Gregory Chanan, Trevor  
 550 Killeen, Zeming Lin, Natalia Gimelshein, Luca Antiga, et al. Pytorch: An imperative style, high-  
 551 performance deep learning library. *Advances in neural information processing systems*, 32, 2019.

552

553 Zhen Peng, Wenbing Huang, Minnan Luo, Qinghua Zheng, Yu Rong, Tingyang Xu, and Junzhou  
 554 Huang. Graph representation learning via graphical mutual information maximization. In *Pro-  
 ceedings of The Web Conference 2020*, pp. 259–270, 2020.

555

556 Jiezhong Qiu, Qibin Chen, Yuxiao Dong, Jing Zhang, Hongxia Yang, Ming Ding, Kuansan Wang,  
 557 and Jie Tang. Gcc: Graph contrastive coding for graph neural network pre-training. In *Pro-  
 ceedings of the 26th ACM SIGKDD international conference on knowledge discovery & data mining*,  
 558 pp. 1150–1160, 2020.

559

560 Yu Rong, Wenbing Huang, Tingyang Xu, and Junzhou Huang. Dropedge: Towards deep graph  
 561 convolutional networks on node classification. In *International Conference on Learning Repre-  
 sentations*, 2020.

562

563 Prithviraj Sen, Galileo Namata, Mustafa Bilgic, Lise Getoor, Brian Galligher, and Tina Eliassi-Rad.  
 564 Collective classification in network data. *AI magazine*, 29(3):93–93, 2008.

565

566 Oleksandr Shchur, Maximilian Mumme, Aleksandar Bojchevski, and Stephan Günnemann. Pitfalls  
 567 of graph neural network evaluation. *arXiv preprint arXiv:1811.05868*, 2018.

568

569 Xiao Shen, Dewang Sun, Shirui Pan, Xi Zhou, and Laurence T Yang. Neighbor contrastive learning  
 570 on learnable graph augmentation. In *Proceedings of the AAAI conference on artificial intelligence*,  
 volume 37, pp. 9782–9791, 2023.

571

572 Xiao Shen, Zhihao Chen, Shirui Pan, Shuang Zhou, Laurence T Yang, and Xi Zhou. Open-set  
 573 cross-network node classification via unknown-excluded adversarial graph domain alignment. In  
 574 *Proceedings of the AAAI Conference on Artificial Intelligence*, volume 39, pp. 20398–20408,  
 2025.

575

576 Kihyuk Sohn. Improved deep metric learning with multi-class n-pair loss objective. *Advances in  
 577 neural information processing systems*, 29, 2016.

578

579 Yonglong Tian, Chen Sun, Ben Poole, Dilip Krishnan, Cordelia Schmid, and Phillip Isola. What  
 580 makes for good views for contrastive learning? *Advances in neural information processing sys-  
 tems*, 33:6827–6839, 2020.

581

582 Laurens Van der Maaten and Geoffrey Hinton. Visualizing data using t-sne. *Journal of machine  
 learning research*, 9(11), 2008.

583

584 Petar Velickovic, Guillem Cucurull, Arantxa Casanova, Adriana Romero, Pietro Lio, Yoshua Ben-  
 585 gio, et al. Graph attention networks. *stat*, 1050(20):10–48550, 2017.

586

587 Petar Veličković, William Fedus, William L. Hamilton, Pietro Liò, Yoshua Bengio, and R Devon  
 588 Hjelm. Deep graph infomax. In *International Conference on Learning Representations*, 2019.

589

590 Guancheng Wan, Yijun Tian, Wenke Huang, Nitesh V Chawla, and Mang Ye. S3gcl: Spectral, swift,  
 591 spatial graph contrastive learning. In *Forty-first International Conference on Machine Learning*,  
 2024.

592

593 Sheng Wan, Shirui Pan, Jian Yang, and Chen Gong. Contrastive and generative graph convolutional  
 networks for graph-based semi-supervised learning. In *Proceedings of the AAAI conference on  
 artificial intelligence*, volume 35, pp. 10049–10057, 2021a.

594 Sheng Wan, Yibing Zhan, Liu Liu, Baosheng Yu, Shirui Pan, and Chen Gong. Contrastive graph  
 595 poisson networks: Semi-supervised learning with extremely limited labels. *Advances in Neural*  
 596 *Information Processing Systems*, 34:6316–6327, 2021b.

597 Minjie Wang, Da Zheng, Zihao Ye, Quan Gan, Mufei Li, Xiang Song, Jinjing Zhou, Chao Ma,  
 598 Lingfan Yu, Yu Gai, et al. Deep graph library: A graph-centric, highly-performant package for  
 599 graph neural networks. *arXiv preprint arXiv:1909.01315*, 2019.

600 Jun Xia, Lirong Wu, Ge Wang, Jintao Chen, and Stan Z Li. Progl: Rethinking hard negative mining  
 601 in graph contrastive learning. *arXiv preprint arXiv:2110.02027*, 2021.

602 Teng Xiao, Huaisheng Zhu, Zhengyu Chen, and Suhang Wang. Simple and asymmetric graph  
 603 contrastive learning without augmentations. *Advances in neural information processing systems*,  
 604 36:16129–16152, 2023.

605 Yaochen Xie, Zhao Xu, Jingtun Zhang, Zhengyang Wang, and Shuiwang Ji. Self-supervised learning  
 606 of graph neural networks: A unified review. *IEEE transactions on pattern analysis and machine*  
 607 *intelligence*, 45(2):2412–2429, 2022.

608 Zhilin Yang, William Cohen, and Ruslan Salakhudinov. Revisiting semi-supervised learning with  
 609 graph embeddings. In *International conference on machine learning*, pp. 40–48, 2016.

610 Yihang Yin, Qingzhong Wang, Siyu Huang, Haoyi Xiong, and Xiang Zhang. Autogcl: Automated  
 611 graph contrastive learning via learnable view generators. In *Proceedings of the AAAI conference*  
 612 *on artificial intelligence*, volume 36, pp. 8892–8900, 2022.

613 Zhitao Ying, Jiaxuan You, Christopher Morris, Xiang Ren, Will Hamilton, and Jure Leskovec. Hier-  
 614 archical graph representation learning with differentiable pooling. *Advances in neural information*  
 615 *processing systems*, 31, 2018.

616 Yuning You, Tianlong Chen, Yongduo Sui, Ting Chen, Zhangyang Wang, and Yang Shen. Graph  
 617 contrastive learning with augmentations. *Advances in neural information processing systems*, 33:  
 618 5812–5823, 2020.

619 Hengrui Zhang, Qitian Wu, Junchi Yan, David Wipf, and Philip S Yu. From canonical correlation  
 620 analysis to self-supervised graph neural networks. *Advances in Neural Information Processing*  
 621 *Systems*, 34:76–89, 2021.

622 Hengrui Zhang, Qitian Wu, Yu Wang, Shaofeng Zhang, Junchi Yan, and Philip S Yu. Localized  
 623 contrastive learning on graphs. *arXiv preprint arXiv:2212.04604*, 2022.

624 Hongyuan Zhang, Jiankun Shi, Rui Zhang, and Xuelong Li. Non-graph data clustering via-bipartite  
 625 graph convolution. *IEEE Transactions on Pattern Analysis & Machine Intelligence*, 45(07):8729–  
 626 8742, 2023.

627 Hongyuan Zhang, Yanan Zhu, and Xuelong Li. Decouple graph neural networks: train multiple  
 628 simple gnns simultaneously instead of one. *IEEE Transactions on Pattern Analysis and Machine*  
 629 *Intelligence*, 46(11):7451–7462, 2024a.

630 Jiyang Zhang, Zijing Liu, Yu Wang, Bin Feng, and Yu Li. Subgdiff: A subgraph diffusion model to  
 631 improve molecular representation learning. *Advances in Neural Information Processing Systems*,  
 632 37:29620–29656, 2024b.

633 Liyuan Zhang, Yongquan Jiang, and Yan Yang. Gnng3d: Protein function prediction based on 3d  
 634 structure and functional hierarchy learning. *IEEE Transactions on Knowledge and Data*  
 635 *Engineering*, 36(8):3867–3878, 2024c.

636 Muhan Zhang, Zhicheng Cui, Marion Neumann, and Yixin Chen. An end-to-end deep learning  
 637 architecture for graph classification. In *Proceedings of the AAAI conference on artificial intelli-*  
 638 *gence*, volume 32, 2018.

639 Wenting Zhao, Gongping Xu, Zhen Cui, Siqiang Luo, Cheng Long, and Tong Zhang. Deep graph  
 640 structural infomax. In *Proceedings of the AAAI conference on artificial intelligence*, volume 37,  
 641 pp. 4920–4928, 2023.

648 Ziwen Zhao, Yixin Su, Yuhua Li, Yixiong Zou, Ruixuan Li, and Rui Zhang. A survey on self-  
649 supervised graph foundation models: Knowledge-based perspective. *IEEE Transactions on*  
650 *Knowledge and Data Engineering*, 2025.

651

652 Yanqiao Zhu, Yichen Xu, Feng Yu, Qiang Liu, Shu Wu, and Liang Wang. Deep graph contrastive  
653 representation learning. *arXiv preprint arXiv:2006.04131*, 2020.

654

655 Yanqiao Zhu, Yichen Xu, Feng Yu, Qiang Liu, Shu Wu, and Liang Wang. Graph contrastive learning  
656 with adaptive augmentation. In *Proceedings of the web conference 2021*, pp. 2069–2080, 2021.

657

658 Jiaming Zhuo, Yintong Lu, Hui Ning, Kun Fu, Dongxiao He, Chuan Wang, Yuanfang Guo, Zhen  
659 Wang, Xiaochun Cao, Liang Yang, et al. Unified graph augmentations for generalized contrastive  
660 learning on graphs. *Advances in Neural Information Processing Systems*, 37:37473–37503, 2024.

661

662

663

664

665

666

667

668

669

670

671

672

673

674

675

676

677

678

679

680

681

682

683

684

685

686

687

688

689

690

691

692

693

694

695

696

697

698

699

700

701